



22 estimates, and growth planes between structures are highly correlated with somatic growth. Daily  
23 otolith increment width mirrored the results of the somatic growth study in both structures.  
24 Generally, the lapillus had fewer complications resulting in a better fit to growth and treatment  
25 data, primarily due to the lack of accessory growth centers.

## 26 **Introduction**

27 The abundance of sablefish (*Anoplopoma fimbria*) in the Gulf of Alaska (GOA) has declined  
28 substantially since 1988, with only a few strong year classes supporting the fishery (Hanselman  
29 et al., 2019). Understanding the factors driving year-class success and recruitment can reduce  
30 uncertainty in stock assessment models. The recruitment of Alaska sablefish is believed to be  
31 decoupled from spawning stock biomass and driven by environmental variability (Hanselman et  
32 al., 2019). Previous research has suggested a relationship between large-scale oceanographic  
33 indices and sablefish recruitment in the California Current and off the coast of Vancouver Island,  
34 British Columbia (Coffin and Mueter, 2016; King et al., 2000; Schirripa and Colbert, 2006;  
35 Shotwell et al., 2014; Sigler et al., 2001; Sogard, 2011); however, the relationship between  
36 juvenile sablefish growth/life history, environmental drivers, and recruitment success in Alaska  
37 has not been investigated.

38 Juvenile growth tends to have a positive and predictive relationship with recruitment in many  
39 fishes (Metcalf and Monaghan, 2003), including sablefish in the California Current ecosystem  
40 (Sogard, 2011). Juvenile sablefish growth rates observed under laboratory conditions were  
41 among the fastest recorded for any juvenile marine fish (Sogard, 2011). This accelerated growth  
42 likely comes at a physiological cost, making juvenile sablefish more vulnerable to environmental  
43 fluctuations. Measuring and comparing juvenile sablefish growth between environmental  
44 conditions and in the context of recruitment in the GOA could help identify potential drivers for

45 survival and reduce uncertainty within stock assessment results. The generally accepted “bigger  
46 is better” approach to understanding growth rates and survival in marine fishes lends support to  
47 the strategy of maximizing growth. While the physiological cost of rapid growth may render  
48 fishes more susceptible to environmental conditions, the tradeoff is a reduced period spent within  
49 a smaller, more vulnerable size class (Houde, 1987).

50 Variation in fish growth is reflected in the microstructure of otoliths. Analysis of visible banding  
51 patterns within the otolith structure are used to estimate growth rates, daily age, migration  
52 patterns, and stock structure (Campana, 2005; Panfili et al., 2002). Larval and juvenile otolith  
53 size and growth has been shown to be highly correlated to somatic growth or fish length in other  
54 temperate species (Fey, 2006; Moksness and Wespestad, 1989; Otterlei et al., 2002; Wright et  
55 al., 1990) as well as other fast-growing species (Megalofonou, 2006). For example, lapillus  
56 growth was highly correlated with standard length in larval and early juvenile Atlantic cod, and  
57 otolith growth was linked to temperature effects, providing context for environmental variation  
58 (Otterlei et al., 2002). Previous studies on juvenile sablefish have successfully developed growth  
59 indices using otolith microstructure analysis (Beamish and McFarlane, 1983; Boehlert and  
60 Yoklavich, 1985; Courtney and Severin, 2007; King et al., 2000; Sigler et al., 2001; Sogard,  
61 2011). These studies have shown clear temperature effects on growth in laboratory-reared fish  
62 and correlations between Pacific Decadal Oscillation indices, sea surface height, and Ekman  
63 transport in juvenile sablefish caught in the California Current. Juvenile sablefish have  
64 demonstrated a dome-shaped relationship between temperature and growth (Krieger et al., 2019),  
65 similar to many other species (Hofmann and Fischer, 2003; Takasuka and Aoki, 2006; Xing et  
66 al., 2021). If juvenile otolith increment width is predictive of somatic growth, then you would  
67 expect to see a similar relationship.

68 The microstructure of otoliths consists of concentric layers of relatively protein rich, opaque (D-  
69 zone) and calcium carbonate-rich, translucent (L-zone) material, which form interpretable  
70 bipartite increments representing sub-daily to annual growth periods (Campana, 2001; Panfili et  
71 al., 2002). However, for otolith microstructure to be informative, it must be entrained to cyclical  
72 environmental events or endogenous circadian rhythms that continue, even in the absence of  
73 somatic growth (Geffen, 1987). Otolith growth corresponds to environmental stimuli such as diel  
74 light/dark cycles (daily increments), seasonal growth patterns (temperature and food  
75 availability), and inter-annual patterns which are reflected in the degree of opacity and amount of  
76 material accreted to the otolith (Høie et al., 2008). Areas of discontinuity in fish otoliths (check  
77 marks) typically denote stress, or large thermal changes, such as those used for thermal marking  
78 in hatcheries (Volk et al., 1999). The incidence of sub-daily increments tends to increase during  
79 periods of rapid growth, complicating the interpretation of daily increment patterns (Stevenson  
80 and Campana, 1993). These increments can typically be differentiated as they tend to be less  
81 well defined and break up a more normal pattern observed within daily increments (Stevenson  
82 and Campana, 1993). Studying these interpretable patterns and their relationship to internal and  
83 external stimuli can give insights into the conditions experienced during the life of an individual  
84 and the impacts of varying environmental conditions on fish health.

85 Otolith microstructure can be used to examine recruitment dynamics of sablefish (Beamish and  
86 McFarlane, 1983; Boehlert and Yoklavich, 1985; Courtney and Severin, 2007; King et al., 2000;  
87 Sigler et al., 2001; Sogard, 2011), but a clear understanding of the relationship between otolith  
88 and somatic growth is needed. To accurately estimate daily age, otoliths need to have an  
89 identifiable hatch mark and the daily formation of increments needs to be validated. The hatch  
90 mark (Deary et al., 2019) and daily increments of sablefish have been validated for the sagittal

91 otolith (Courtney and Severin, 2007). Issues with processing and measuring sablefish sagittal  
92 otoliths include the presence of accessory growth centers (e.g., accessory primordia as defined in  
93 Panfili et al., 2002) and the convex shape of the otolith (Courtney & Severin, 2007). Lapillar  
94 otoliths have also been used to investigate individual responses to stimuli (Sogard, 2011). The  
95 lapillus may not form accessory growth centers, but the method has not been validated for daily  
96 age. Given the potential utility of both structures and the resulting data, a comparison and  
97 evaluation of structures and growth is warranted.

98 The objectives for this study were as follows:

- 99 1. Compare daily age estimates from the lapillus and sagitta to provide a corroboration for daily  
100 increment periodicity for lapillar otoliths using a validated structure.
- 101 2. Compare otolith dimensions to fish length to investigate the relationship between otolith  
102 growth and somatic growth.
- 103 3. Compare mean daily increment width with temperature and feeding ration treatments to  
104 investigate their effect on daily increment formation.
- 105 4. Examine the relationship between mean daily somatic growth and mean daily otolith  
106 increment width (sagittal and lapillar) from specimens subjected to temperature and ration  
107 treatments.

## 108 **Methods**

109 Both lapillar and sagittal otoliths were collected from juvenile sablefish sampled in multiple  
110 locations in the eastern Gulf of Alaska (EGOA) during 2014, 2016, and 2017 (Table 1). July and  
111 August samples were collected during the National Marine Fisheries Service (NMFS) EGOA

112 Eastern Gulf of Alaska Ecosystem Assessment Survey (Strasburger et al., 2018). October  
113 otoliths (sagitta only) were collected in Saint John Baptist Bay in Southeast Alaska (Callahan et  
114 al., 2021). Additional juvenile otoliths were sampled from a controlled temperature and feeding  
115 ration growth study conducted at Auke Bay Laboratory /Alaska Fishery Science Center (Krieger  
116 et al., 2019). A detailed description of the experimental design is available within Krieger et al.,  
117 2019 and 2020. Briefly, juvenile sablefish were randomly assigned to one of four temperature  
118 treatments combined with one of three ration treatments, resulting in twelve treatment levels.  
119 Temperature treatment levels were 6.5, 12.7, 16.8, and 19.5°C and feeding rations were  $C_{25}$ ,  $C_{50}$ ,  
120  $C_{max}$ . Feeding rations were based on fish weight and consumption data collected during a 2017  
121 feeding trial experiment (Krieger et al., 2019).  $C_{max}$  was feeding to satiation,  $C_{50}$  was feeding at  
122 one half of  $C_{max}$ , and  $C_{25}$  was feeding at one quarter of  $C_{max}$ . Fish were held on a natural photo  
123 period cycle. Due to the small sample size of recoverable otoliths available at the onset of this  
124 study, we rely on results from Krieger et al., 2019 and 2020 in finding no tank effect with a  
125 larger sample size. Juveniles from this growth study were originally sampled during the 2017  
126 EGOA survey (Strasburger et al., 2018). Treatment levels, and individual mean daily growth  
127 (mm/day FL) from Krieger et al., 2019, were used with permission for further analyses.  
128

129 Sagittal and lapillar otoliths were mounted to petrographic slides using Crystalbond™ 509  
130 thermal plastic cement and whole otolith images (Figure 1) were taken using a LeicaMZ6  
131 stereoscopic microscope with a Leica DFC450 camera at 1.25-4.0× magnification with reflected  
132 lighting. Images were taken using Image-Pro Premiere® 9.3 software. After the whole otolith  
133 was imaged, the distal and proximal surface of the otoliths were polished using Buehler 1200 grit  
134 (P2400) micro-cut silicon carbide grinding paper and 0.3-micron FibrMet abrasive discs. After

135 the distal surface of the otolith was ground, the slide was heated on a hot plate and the otolith  
136 was flipped and remounted on its distal side. The proximal side of the otolith was then ground  
137 until the nucleus and daily growth increments were visible.

138 After daily growth increments and the nucleus were visible, images were taken of otoliths using  
139 a Leica DMLS compound microscope, DFC450C camera at 6.3×, 12.3×, 25.2×, and 63×  
140 magnification with both air and oil immersion objectives and single- or double-polarization.  
141 Image-Pro Premier® and Image-Pro® were used to measure the whole otolith and daily growth  
142 increments. For whole otoliths, linear measurements were collected along anterior-posterior  
143 (length), dorsal-ventral (height), and nucleus to common feature transects to investigate  
144 otolith/fish size relationships and to corroborate daily increment count and measurement results  
145 (Figure 2). For daily growth increment counts and measurements, the primordium were  
146 identified, the hatch mark was marked as the beginning of the first daily increment, and a  
147 transect was drawn from the primordia to the edge of the otolith. Daily increments were defined  
148 as a pair of continuous, consecutive light/dark bands, where the darkest part (typically the middle  
149 of the dark zone) was labeled as the start/stop of an increment. Transects were drawn where the  
150 most consecutive increments were visible. Daily increment measurements from otoliths collected  
151 from fish included in the temperature/feeding ration growth study were restricted to the last 30  
152 days of the study to ensure increments were the result of each treatment. Temperature and ration  
153 treatments were not sampled evenly due to mortality events during the growth trial (Table 1).

154 Daily increment counts from the lapillus and sagitta were compared (Figure 3) to investigate  
155 lapillar otolith utility for daily age estimation. A linear regression comparing sagittal and lapillar  
156 daily increments was calculated as:

157 
$$SDA_i = \beta_0 + \beta_1 \cdot LPA_i + \varepsilon_i ,$$

158 where  $SDA_i$  was the sagittal daily age estimate,  $LPA_i$  was the lapillar daily age estimate,  $\beta_0$  was  
159 the intercept,  $\beta_1$  is the slope, and  $\varepsilon_i$  was the error. McNemar, Evans-Hoenig, and Bowker bias  
160 tests were completed, as suggested by (McBride, 2015). Daily age estimation methods were  
161 considered comparable if the linear model and bias tests did not suggest significant bias between  
162 ages.

163 Linear models were also used to compare linear otolith measurements to fish length (Figure 4).  
164 Based on initial fish length to otolith size comparisons and to target the axis where daily  
165 increments were counted and measured, the lapillus diameter and sagitta height were used for  
166 modeling. The significance of linear relationships between otolith and fish size were used to test  
167 whether otolith growth could be used as a proxy for fish growth:

168 
$$FL_i = \beta_0 + \beta_1 \cdot D_i + \varepsilon_i ,$$

169 where  $FL_i$  was the individual fish fork-length (mm),  $D_i$  was either lapillus diameter or sagitta  
170 height ( $\mu\text{m}$ ),  $\beta_0$ s were the estimated intercepts for each respective model, and  $\beta_1$ s were the  
171 estimated slope coefficients for each respective model, and  $\varepsilon_i$  was the error.

172 Separate quadratic models for lapillus and sagittal otoliths were used to evaluate the effects of  
173 temperature and feeding ration on mean daily increment width over the study period:

174 
$$Inc_{iTR} = \beta_1 \cdot Temp + \beta_2 \cdot Temp^2 + \varepsilon_{iTR}$$

175 where  $Inc_{iTR}$  is the average increment width ( $\mu\text{m}$ ) at temperature T and ration R for specimen  $i$ ,  
176  $Temp$  is the temperature treatment ( $^{\circ}\text{C}$ ), and  $\varepsilon_{iTR}$  was the individual specimen treatment error  
177 (Figure 5).



178 Lastly, we tested for differences in the slope of the relationship between mean observed growth  
179 rates from Krieger et al., (2019) and mean increment widths from each structure, temperature  
180 and feeding ration group using fitted linear models (Figures 6 & 7), and an anova. If the  
181 interaction term between mean increment width and either treatment group (temperature or  
182 ration) was significant, the slope was deemed to be significantly different for that respective  
183 structure (sagitta or lapillus). All statistical analyses were completed using RStudio (Ogle, 2016;  
184 R Core Team, 2019), all R code and original/reproduced data used to produce the preceding  
185 models, tests, and referenced figures are available at the public url:

186 <https://github.com/Strasburger/Sablefish-Otolith-Utility>

## 187 **Results**

188 Ages were between 105 and 160 days from hatch and daily age counts were similar between  
189 lapillar and sagittal otoliths (mean difference between paired ages was  $-0.23 \text{ days} \pm 3.39 \text{ SD}$ ;  
190 Figure 3). A linear model suggested no significant difference between paired structure age  
191 estimates ( $p = 0.00$ ,  $df = 20$ ). Bias tests support the linear model results and were not significant  
192 (McNemar:  $p = 0.80$ ; Evans-Hoenig:  $p = 0.87$ ; Bowker:  $p = 0.45$ ). These findings support the use  
193 of either otolith for daily age estimation (Figure 3). Further, there were strong linear trends  
194 between fish length and lapillar and sagittal otolith measurements (lapillus:  $p < 0.01$ ; sagitta:  $p <$   
195  $0.01$ ; Figure 4), suggesting that otolith growth could be used as a proxy for somatic growth.

196 Quadratic models of both lapillar and sagittal otolith daily increment width and  
197 temperature/feeding treatments were significant (lapillus:  $p < 0.01$ ; sagitta:  $p < 0.01$ ). Both  
198 models suggested that peak daily increment width occurred at approximately  $13^{\circ}\text{C}$  and at the  
199 maximum feed ration ( $C_{\text{max}}$ ; Figure 5); however, the lapillus model explained a greater

200 proportion of the variance (adjusted  $r^2 = 0.90$  vs.  $0.60$  for the sagitta model). Both the quadratic  
201 coefficients and the interaction terms (temperature and ration) were significant ( $p < 0.01$ ).  
202 Though sample sizes were not uniform across treatments due to fish survival in extreme  
203 treatments (Table 1), dome-shaped relationship between temperature and otolith increment width  
204 mirrors the growth trends in the previous study (Krieger et al., 2019).

205 The linear relationships between mean daily increment width and mean daily growth (lapillus:  $p$   
206  $< 0.01$ ; sagitta:  $p < 0.01$ ) provide further support that somatic growth and otolith growth are  
207 coupled in juvenile sablefish (Figures 6 & 7). The slope of this relationship remained similar  
208 across feeding rations for both otolith structures, but varied at the extreme temperature  
209 treatments, suggesting that the temperature effect is stronger than the ration effect across the  
210 range of treatments tested. The interaction term between average increment width and  
211 temperature was significant for the lapillus only ( $p < 0.03$ ), there were no significant interactions  
212 between increment width and ration for either otolith structure. This suggests that there may be a  
213 temperature threshold after which the relationship between somatic and otolith growth changes.

## 214 **Discussion**

215 The findings presented here support the utility of both the lapillar and sagittal otolith to assess  
216 growth in juvenile sablefish. Daily age estimates from the lapillus and sagitta were highly  
217 correlated, suggesting that both otoliths record daily age in juvenile sablefish, given previous  
218 validation on sagittal otoliths (Courtney and Severin, 2007; Deary et al., 2019). Further, the  
219 strong linear relationship between otolith dimensions and somatic length, and the effects of  
220 temperature and feed ration on otolith growth support past and future use of lapillar and sagittal  
221 otoliths for modeling juvenile sablefish growth in changing environments.

222 The quadratic relationship between temperature and otolith increment width within feeding  
223 ration treatments agrees with the growth response published in Krieger et al. (2019) using the  
224 same specimens. However, interpretation of otolith model results should be done with care. The  
225 otolith-somatic growth relationship may decouple at temperature extremes, suggested by the  
226 changes in slope detected across temperature treatment between mean somatic growth and mean  
227 otolith increment width (Figure 6). This concern may be marginal due to the extreme  
228 temperature treatment (19.5°C), which is not likely to occur in the GOA. Further, the  
229 relationship between temperature and increment width was relatively stable across temperatures  
230 commonly experienced by wild juvenile sablefish (Strasburger et al., 2018).

231 Although either structure may be used to reliably estimate daily age in juvenile sablefish, some  
232 thought should be exercised in the selection of which otolith to examine. The sagitta is larger,  
233 more easily identified, and more manageable initially; however, they have numerous accessory  
234 growth centers (Courtney & Severin, 2007). These growth centers are the most common  
235 distortion in the shape of early otoliths in marine fish, which are usually associated with the end  
236 of the transformation from larvae to juveniles (Panfili et al., 2002). In addition, the crenulations  
237 along the dorsal margin can distort increment widths and make following a consistent  
238 counting/measurement transect difficult. These factors introduce the possibility of losing  
239 information using a sagittal plane preparation and may produce lower quality preparations and  
240 imprecise counts and measurements. Conversely, the lapillus is more difficult to excise and  
241 manipulate prior to mounting to a slide; however, accessory growth centers were not an issue,  
242 the growth and margins were more uniform, and increment width measurement axes were more  
243 consistent. Both otoliths exhibited sub-daily increments. Caution should be exercised in the  
244 preparation and imaging of juvenile sablefish otoliths. These increments can be differentiated

245 with experience, and future work should evaluate criteria for defining daily increments to assess  
246 the accuracy of data.

247 The overarching objective of this study was to understand the relationship between otolith and  
248 somatic growth in juvenile sablefish. Results indicated that otolith microstructure can be used to  
249 examine connections between juvenile sablefish growth, changing temperature and prey field  
250 conditions, and potential subsequent recruitment success. Evidence from previous studies  
251 suggests that growth of juvenile sablefish has the potential to be predictive of year class success.  
252 The results presented here support these previous studies and further inform the relationship  
253 between somatic growth, otolith growth, and temperature and prey field conditions needed to  
254 produce growth models from the daily increments of juvenile sablefish otoliths.

255 Growth in juvenile sablefish correlates with local temperatures and large-scale climate variability  
256 (Sogard and Olla, 1998). Juvenile sablefish growth in the California Current system was  
257 correlated to the monthly Pacific Decadal Oscillation (PDO) index, sea surface height, and  
258 Ekman transport (Sogard, 2011). A persistent Aleutian low, above average southwesterly winds,  
259 and warmer coastal sea surface temperature in the Northeast Pacific were correlated to an  
260 increased average year-class survival and decadal patterns in the relative success of sablefish off  
261 Vancouver Island, British Columbia (King et al., 2000). Laboratory-reared juvenile sablefish (30  
262 – 50 mm total length) exhibited a rapid rise in daily growth rates between 6 and 14° C, a gradual  
263 rise between 14 and 22° C, and a precipitous drop at 24° C (Sogard and Olla, 2001). Similar  
264 results were observed in a laboratory study using larger (220 – 290 mm total length) juveniles  
265 (Krieger et al., 2019). Conversion efficiency of food ration into somatic tissue in juvenile  
266 sablefish increases with temperature under both low and high daily ration, albeit at different rates  
267 (Sogard and Olla, 2001). This indicates that temperature has a benefit to juvenile sablefish

268 growth, even in the presence of sub-optimal prey conditions (Sogard & Olla, 2001), as observed  
269 in this study. Results described here and by Krieger et al. (2019) suggest an optimal temperature  
270 window for juvenile sablefish growth in the Gulf of Alaska.

271 Juvenile length was selected for this analysis because otolith growth is likely to be related to  
272 structural growth (i.e length) in fishes. While in some cases, energy density (commonly linked to  
273 the likelihood of overwinter survival) may be predicted with weight, particularly percent dry  
274 weight, length is more appropriate for juvenile fishes that store energy as proteins (Bavčević et  
275 al., 2020; Krieger et al., 2020; Sogard and Spencer, 2004). Sablefish do not begin to accumulate  
276 lipids until approximately age-3 (AFSC, unpublished data). In addition, juvenile sablefish weight  
277 predictably and reliably increases as a cubic function of length, a relationship that holds well  
278 beyond their first year (Harvey et al., 2000). Describing the relationship between juvenile  
279 somatic growth in terms of length and otolith growth, in effect, also describes the relationship  
280 between fish somatic growth in terms of weight and otolith growth. However, structural growth  
281 (length) is the metric most often associated with predator avoidance and the ability to capture  
282 larger and more efficient prey (Sogard, 1997). Finally, many of the archived and continuously  
283 collected samples available for juvenile sablefish were collected at sea or in remote field sites  
284 where the accurate measurement of weight is often a challenge. Length can be quickly and  
285 accurately assessed while samples are fresh, while any preservation method is likely to affect  
286 water weight of the sample (Baltasar et al., 2021).

287 Recent conditions in the Gulf of Alaska (the persistent oceanic heatwave known as “the Blob”,  
288 persistent El Niño) had observable effects on the temperature experienced by juvenile sablefish  
289 and prey availability in their first summer. Sea surface temperatures have persistently had  
290 maximums around 15-16° C from 2014 to 2017 (Litzow et al., 2020; Strasburger et al., 2018).

291 These maximum temperatures coincide with observed maximum growth rates within laboratory  
292 settings (Krieger et al., 2019; Sogard, 2011). Further, prey abundance has shifted recently in the  
293 Gulf of Alaska, and zooplankton communities have been predominantly gelatinous species and  
294 small copepods (Batten et al., 2022; Pinchuk et al., 2021; Strasburger et al., 2018). Copepods and  
295 copepod nauplii are important prey for early sablefish larvae (Grover & Olla, 1990; Grover & Olla,  
296 1987). If potential higher growth rates due to increased temperatures are sustainable within the  
297 context of shifting prey fields, and juvenile sablefish benefit from the increased size at age,  
298 measuring Alaska juvenile sablefish growth rates and tracking these across cohorts could be an  
299 important metric for estimating subsequent recruitment. Further, understanding the factors  
300 driving year-class success and recruitment would reduce uncertainty in stock assessment models.

301 This work supports the use of otolith microstructure to examine linkages between wild juvenile  
302 sablefish growth to environmental and ecological conditions experienced during their first year.  
303 Given the relationship between otolith dimensions and fish length, otolith increment width and  
304 temperature/feeding ration, and the relationship between observed somatic growth and daily  
305 increment width, it is reasonable to reconstruct daily growth histories for juvenile sablefish from  
306 the Gulf of Alaska, and to relate those growth histories to covariates such as temperature and  
307 prey availability.

### 308 **Acknowledgments**

309 This work was funded through the National Cooperative Research Program, administered by the  
310 Alaska Fisheries Science Center. The authors would like to thank J. Murphy for his discussions  
311 on the preparation and interpretation of the microstructure of juvenile fish otoliths, as well as  
312 providing a review of the manuscript. We also thank the vessel and scientific crew during the  
313 Eastern Gulf of Alaska surveys for the collection of samples for this project. The findings and

314 conclusions in the paper are those of the author(s) and do not necessarily represent the views of  
315 the National Marine Fisheries Service. Reference to trade names does not imply endorsement by  
316 the National Marine Fisheries Service, NOAA.

## 317 Citations

- 318 Baltasar, R.Q., Burge, E.J., Crane, D.P., 2021. Effects of Frozen Storage on Fish Wet Weight, Percent Dry  
319 Weight, and Length Revisited. *N Am J Fish Manag* 41. <https://doi.org/10.1002/nafm.10691>
- 320 Batten, S.D., Ostle, C., H elaou et, P., Walne, A.W., 2022. Responses of Gulf of Alaska plankton  
321 communities to a marine heat wave. *Deep Sea Research Part II: Topical Studies in Oceanography*  
322 195, 105002. <https://doi.org/10.1016/J.DSR2.2021.105002>
- 323 Bav cevi c, L., Petrovi c, S., Karamarko, V., Luzzana, U., Klanj c cek, T., 2020. Estimating fish energy content  
324 and gain from length and wet weight. *Ecol Modell* 436, 109280.  
325 <https://doi.org/10.1016/J.ECOLMODEL.2020.109280>
- 326 Beamish, R.J., McFarlane, G.A., 1983. The Forgotten Requirement for Age Validation in Fisheries Biology.  
327 *Trans Am Fish Soc* 112, 735–743. [https://doi.org/10.1577/1548-  
328 8659\(1983\)112<735:tfrfav>2.0.co;2](https://doi.org/10.1577/1548-8659(1983)112<735:tfrfav>2.0.co;2)
- 329 Boehlert, G.W., Yoklavich, M.M., 1985. Larval and juvenile growth of sablefish, *Anoplopoma fimbria*, as  
330 determined from otolith increments. *Fishery Bulletin* 83, 475–481.
- 331 Callahan, M.W., Beaudreau, A.H., Heintz, R.A., Mueter, F.J., Rogers, M.C., 2021. Temporal and Age-Based  
332 Variation in Juvenile Sablefish Diet Composition and Quality: Inferences from Stomach Contents  
333 and Stable Isotopes. *Marine and Coastal Fisheries* 13, 396–412.  
334 <https://doi.org/10.1002/MCF2.10173>
- 335 Campana, S.E., 2005. Otolith science entering the 21st century 56, 485–495.  
336 <https://doi.org/10.1071/MF04147>
- 337 Campana, S.E., 2001. Accuracy, precision and quality control in age determination, including a review of  
338 the use and abuse of age validation methods. *J Fish Biol* 59, 197–242.  
339 <https://doi.org/10.1006/jfbi.2001.1668>
- 340 Coffin, B., Mueter, F., 2016. Environmental covariates of sablefish (*Anoplopoma fimbria*) and Pacific  
341 ocean perch (*Sebastes alutus*) recruitment in the Gulf of Alaska. *Deep Sea Research Part II: Topical  
342 Studies in Oceanography* 132, 194–209. <https://doi.org/10.1016/J.DSR2.2015.02.016>
- 343 Courtney, D.L., Severin, K.P., 2007. Validation of otolith increment daily periodicity in captive juvenile  
344 sablefish (*Anoplopoma fimbria*) experimentally immersed in strontium chloride (SrCl<sub>2</sub>). *Fish Res* 83,  
345 246–252. <https://doi.org/10.1016/j.fishres.2006.10.013>

346 Deary, A.L., Porter, S.M., Dougherty, A.B., Duffy-Anderson, J.T., 2019. Preliminary observations of the  
347 skeletal development in pre-flexion larvae of sablefish *Anoplopoma fimbria*. *Ichthyol Res* 66, 177–  
348 182. <https://doi.org/10.1007/s10228-018-0657-0>

349 Fey, D.P., 2006. The effect of temperature and somatic growth on otolith growth: The discrepancy  
350 between two clupeid species from a similar environment. *J Fish Biol* 69.  
351 <https://doi.org/10.1111/j.1095-8649.2006.01151.x>

352 Geffen, A., 1987. Methods of validating daily increment deposition in otoliths of larval fish. In “The Age  
353 and Growth of Fish.”

354 Grover, J.J., Olla, B.L., 1990. Food habits of larval sablefish *Anoplopoma fimbria* from the Bering Sea.  
355 *Fishery Bulletin* 88, 811–814.

356 Grover, J.J., Olla, B.L., 1987. Effects of an El Nino event on the food habits of larval sablefish,  
357 *Anoplopoma fimbria*, off Oregon and Washington. *Fishery Bulletin* 85, 71–79.

358 Hanselman, D.H., Rodgveller, C.J., Fenske, K.H., Shotwell, S.K., Echave, K.B., Malecha, P.W., Lunsford,  
359 C.R., 2019. 3. Assessment of the Sablefish stock in Alaska Executive Summary Summary of Changes  
360 in Assessment Inputs Summary of Results.

361 Harvey, J.T., Loughlin, T.R., Perez, M.A., Oxman, D.S., 2000. Relationship between fish size and otolith  
362 length for 63 species of fishes from the Eastern North Pacific Ocean.  
363 <http://aquaticcommons.org/id/eprint/2511>.

364 Hofmann, N., Fischer, P., 2003. Impact of temperature on food intake and growth in juvenile burbot. *J*  
365 *Fish Biol* 63. <https://doi.org/10.1046/j.1095-8649.2003.00252.x>

366 Høie, H., Folkvord, A., Mosegaard, H., Li, L., Clausen, L.A.W., Norberg, B., Geffen, A.J., 2008. Restricted  
367 fish feeding reduces cod otolith opacity. *Journal of Applied Ichthyology* 24, 138–143.  
368 <https://doi.org/10.1111/j.1439-0426.2007.01014.x>

369 Houde, E.D., 1987. Fish Early Life Dynamics and Recruitment Variability, in: American Fisheries Society  
370 Symposium.

371 King, J.R., Mcfarlane, G.A., Beamish, R.J., 2000. Decadal-scale patterns in the relative year class success  
372 of sablefish (*Anoplopoma fimbria*). *Fish Oceanogr* 9, 62–70. [https://doi.org/10.1046/j.1365-  
373 2419.2000.00122.x](https://doi.org/10.1046/j.1365-2419.2000.00122.x)

374 Krieger, J.R., Beaudreau, A.H., Heintz, R.A., Callahan, M.W., 2020. Growth of young-of-year sablefish  
375 (*Anoplopoma fimbria*) in response to temperature and prey quality: Insights from a life stage  
376 specific bioenergetics model. *J Exp Mar Biol Ecol* 526, 151340.  
377 <https://doi.org/10.1016/J.JEMBE.2020.151340>

378 Krieger, J.R., Sreenivasan, A., Heintz, R., 2019. Temperature-dependent growth and consumption of  
379 young-of-the-year sablefish *Anoplopoma fimbria*: Too hot, too cold or just right? *Fish Res* 209, 32–  
380 39. <https://doi.org/10.1016/j.fishres.2018.09.005>

381 Litzow, M.A., Hunsicker, M.E., Ward, E.J., Anderson, S.C., Gao, J., Zador, S.G., Batten, S., Dressel, S.C.,  
382 Duffy-Anderson, J., Fergusson, E., Hopcroft, R.R., Laurel, B.J., O'Malley, R., 2020. Evaluating



383 ecosystem change as Gulf of Alaska temperature exceeds the limits of preindustrial variability. *Prog*  
384 *Oceanogr* 186. <https://doi.org/10.1016/J.POCEAN.2020.102393>

385 McBride, R.S., 2015. Diagnosis of paired age agreement: a simulation of accuracy and precision effects.  
386 *ICES Journal of Marine Science* 72, 2149–2167. <https://doi.org/10.1093/ICESJMS/FSV047>

387 Megalofonou, P., 2006. Comparison of otolith growth and morphology with somatic growth and age in  
388 young-of-the-year bluefin tuna. *J Fish Biol* 68. <https://doi.org/10.1111/j.1095-8649.2006.01078.x>

389 Metcalfe, N.B., Monaghan, P., 2003. Growth versus lifespan: Perspectives from evolutionary ecology.  
390 *Exp Gerontol* 38, 935–940. [https://doi.org/10.1016/S0531-5565\(03\)00159-1](https://doi.org/10.1016/S0531-5565(03)00159-1)

391 Moksness, E., Wespestad, V., n.d. Ageing and Back-Calculating Growth Rates of Pacific Herring, *Clupea*  
392 *pallasii*, Larvae by Reading Daily Otolith Increments.

393 Ogle, D.H., 2016. *Introductory Fisheries Analyses with R*, *Introductory Fisheries Analyses with R*.  
394 <https://doi.org/10.1111/jfb.13153>

395 Otterlei, E., Folkvord, A., Nyhammer, G., 2002. Temperature dependent otolith growth of larval and  
396 early juvenile Atlantic cod (*Gadus morhua*). *ICES Journal of Marine Science*.  
397 <https://doi.org/10.1006/jmsc.2001.1300>

398 Panfili, J., Pontual, H., Troadec, H., Wright, P.J., 2002. *MANUAL OF FISH SCLEROCHRONOLOGY*. Brest,  
399 France.

400 Pinchuk, A.I., Batten, S.D., Strasburger, W.W., 2021. Doliolid (Tunicata, Thaliacea) Blooms in the  
401 Southeastern Gulf of Alaska as a Result of the Recent Marine Heat Wave of 2014–2016. *Front Mar*  
402 *Sci* 8. <https://doi.org/10.3389/fmars.2021.625486>

403 R Core Team, 2019. *R: A language and environment for statistical computing*. R Foundation for Statistical  
404 Computing.

405 Schirripa, M.J., Colbert, J.J., 2006. Interannual changes in sablefish (*Anoplopoma fimbria*) recruitment in  
406 relation to oceanographic conditions within the California Current System. *Fish Oceanogr* 15, 25–  
407 36. <https://doi.org/10.1111/j.1365-2419.2005.00352.x>

408 Shotwell, S.K., Hanselman, D.H., Belkin, I.M., 2014. Toward biophysical synergy: Investigating advection  
409 along the Polar Front to identify factors influencing Alaska sablefish recruitment. *Deep Sea Res 2*  
410 *Top Stud Oceanogr* 107, 40–53. <https://doi.org/10.1016/J.DSR2.2012.08.024>

411 Sigler, M.F., Rutecki, T.L., Courtney, D.L., Karinen, J.F., Yang, M.-S., 2001. Young of the Year Sablefish  
412 Abundance, Growth, and Diet in the Gulf of Alaska. *Alaska Fishery Research Bulletin* 8, 57–70.

413 Sogard, S.M., 2011. Interannual variability in growth rates of early juvenile sablefish and the role of  
414 environmental factors. *Bull Mar Sci* 87, 857–872. <https://doi.org/10.5343/bms.2010.1045>

415 Sogard, S.M., 1997. Size-selective mortality in the juvenile stage of teleost fishes: A review. *Bull Mar Sci*  
416 60, 1129–1157.

417 Sogard, S.M., Olla, B.L., 2001. Growth and behavioral responses to elevated temperatures by juvenile  
418 sablefish *Anoplopoma fimbria* and the interactive role of food availability. *Mar Ecol Prog Ser* 217,  
419 121–134. <https://doi.org/10.3354/MEPS217121>

420 Sogard, S.M., Olla, B.L., 1998. Behavior of juvenile sablefish, *Anoplopoma fimbria* (Pallas), in a thermal  
421 gradient: Balancing food and temperature requirements. *J Exp Mar Biol Ecol* 222, 43–58.  
422 [https://doi.org/10.1016/S0022-0981\(97\)00137-8](https://doi.org/10.1016/S0022-0981(97)00137-8)

423 Sogard, S.M., Spencer, M.L., 2004. Energy allocation in juvenile sablefish: effects of temperature, ration  
424 and body size. *J Fish Biol* 64, 726–738. <https://doi.org/10.1111/J.1095-8649.2004.00342.X>

425 Stevenson, D.K., Campana, S.E., 1993. Otolith microstructure examination and analysis, *ICES Journal of*  
426 *Marine Science*. <https://doi.org/10.1006/jmsc.1993.1053>

427 Strasburger, W.W., Moss, J.H., Siwicke, K.A., Yasumiishi, E.M., Pinchuk, A.I., Fenske, K.H., 2018. Eastern  
428 Gulf of Alaska Ecosystem Assessment, July through August 2017. NOAA Technical Memorandum.  
429 <https://doi.org/10.7289/V5/TM-AFSC-367>

430 Takasuka, A., Aoki, I., 2006. Environmental determinants of growth rates for larval Japanese anchovy  
431 *Engraulis japonicus* in different waters. *Fish Oceanogr* 15. [https://doi.org/10.1111/j.1365-](https://doi.org/10.1111/j.1365-2419.2005.00385.x)  
432 [2419.2005.00385.x](https://doi.org/10.1111/j.1365-2419.2005.00385.x)

433 Volk, E.C., Schroder, S.L., Grimm, J.J., 1999. Otolith thermal marking, in: *Fisheries Research*.  
434 [https://doi.org/10.1016/S0165-7836\(99\)00073-9](https://doi.org/10.1016/S0165-7836(99)00073-9)

435 Wright, P.J., Metcalfe, N.B., Thorpe, J.E., 1990. Otolith and somatic growth rates in Atlantic salmon parr,  
436 *Salmo salar* L: evidence against coupling. *J Fish Biol* 36. [https://doi.org/10.1111/j.1095-](https://doi.org/10.1111/j.1095-8649.1990.tb05599.x)  
437 [8649.1990.tb05599.x](https://doi.org/10.1111/j.1095-8649.1990.tb05599.x)

438 Xing, Q., Yu, Haiqing, Ito, S. ichi, Ma, S., Yu, Huaming, Wang, H., Tian, Y., Sun, P., Liu, Y., Li, J., Ye, Z., 2021.  
439 Using a larval growth index to detect the environment-recruitment relationships and its linkage  
440 with basin-scale climate variability: A case study for Japanese anchovy (*Engraulis japonicus*) in the  
441 Yellow Sea. *Ecol Indic* 122. <https://doi.org/10.1016/j.ecolind.2020.107301>

442

Figures:

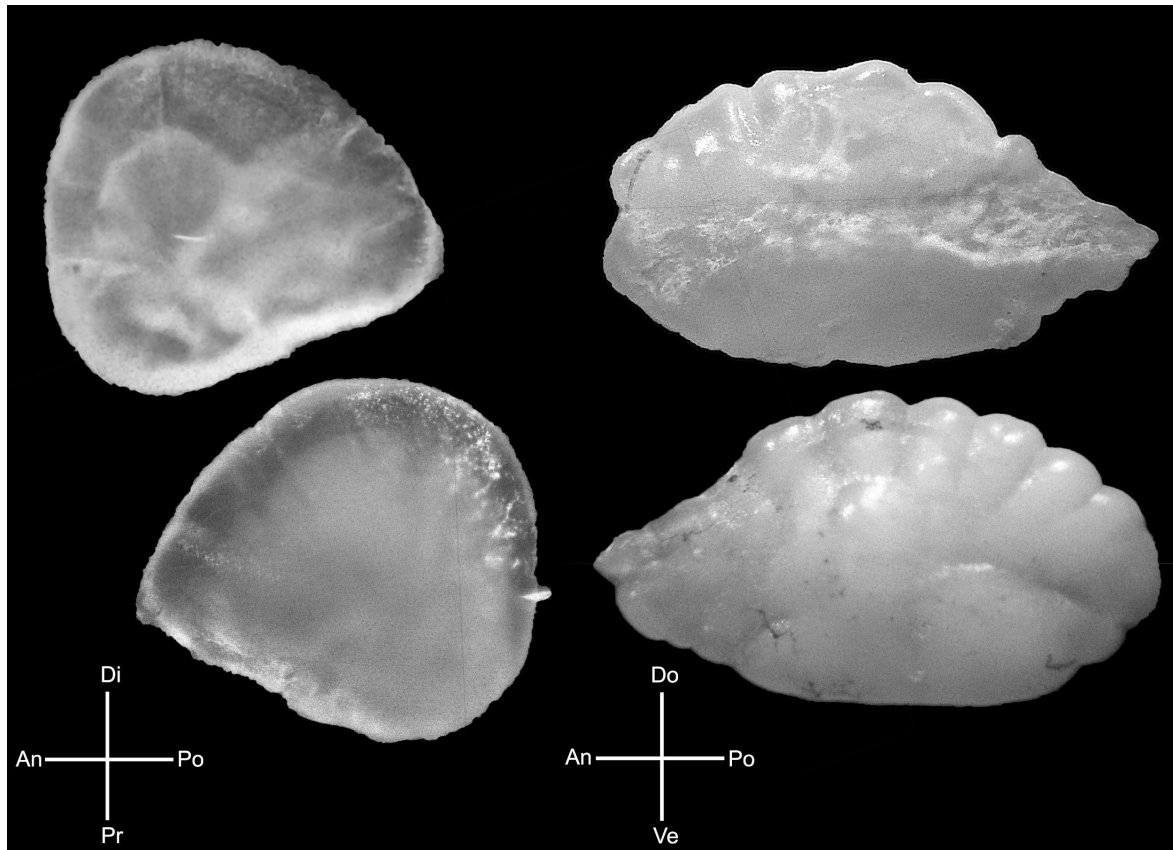


Figure 1. Lapillar (left) and sagittal (right) otoliths from a juvenile sablefish. The top row shows the dorsal lapillar and proximal sagittal otolith surface, and the bottom row shows the ventral lapillar and distal sagittal otolith surface. Keys refer to distal (Di), proximal (Pr), dorsal (Do), ventral (Ve), anterior (An), and posterior (Po). Due to the large variation in otolith size a scale bar was not included. Lapillar diameter ranged from 300 – 900  $\mu\text{m}$ , sagittal height ranged from 450 – 2600  $\mu\text{m}$ .

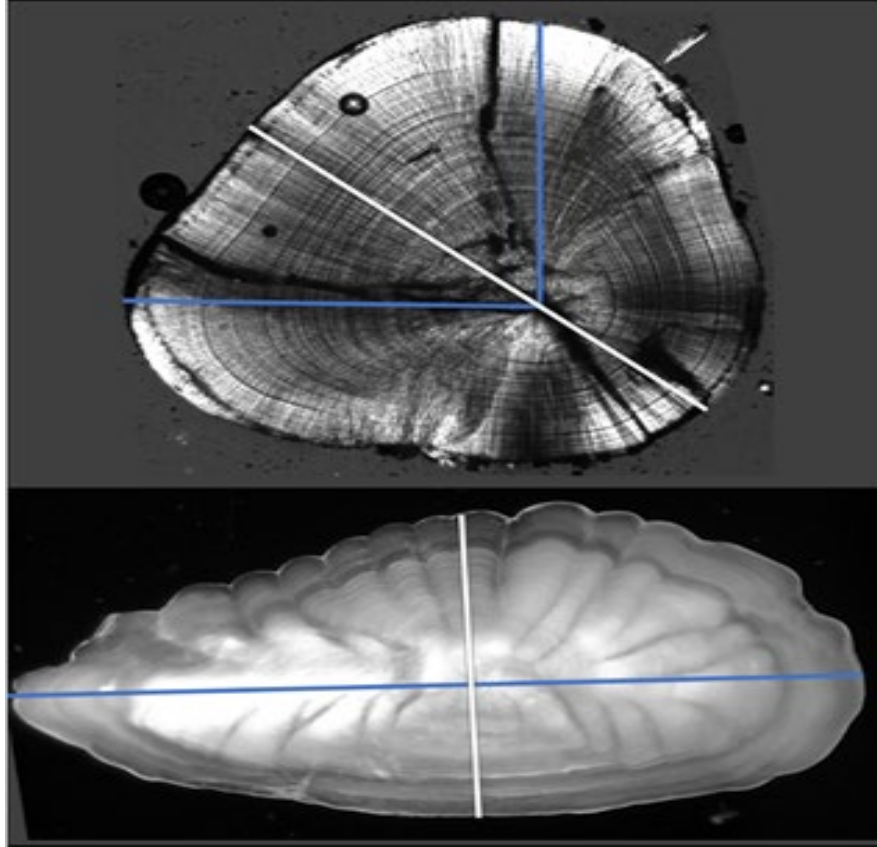


Figure 2. Juvenile sablefish lapillar (top) and sagittal (bottom) otoliths. White lines indicate lapillus diameter and sagitta height used in final otolith-fish size models, blue lines indicate other transects considered. Due to the large variation in otolith size a scale bar was not included. Lapillar diameter ranged from 300 – 900  $\mu\text{m}$ , sagittal height ranged from 450 – 2600  $\mu\text{m}$ .

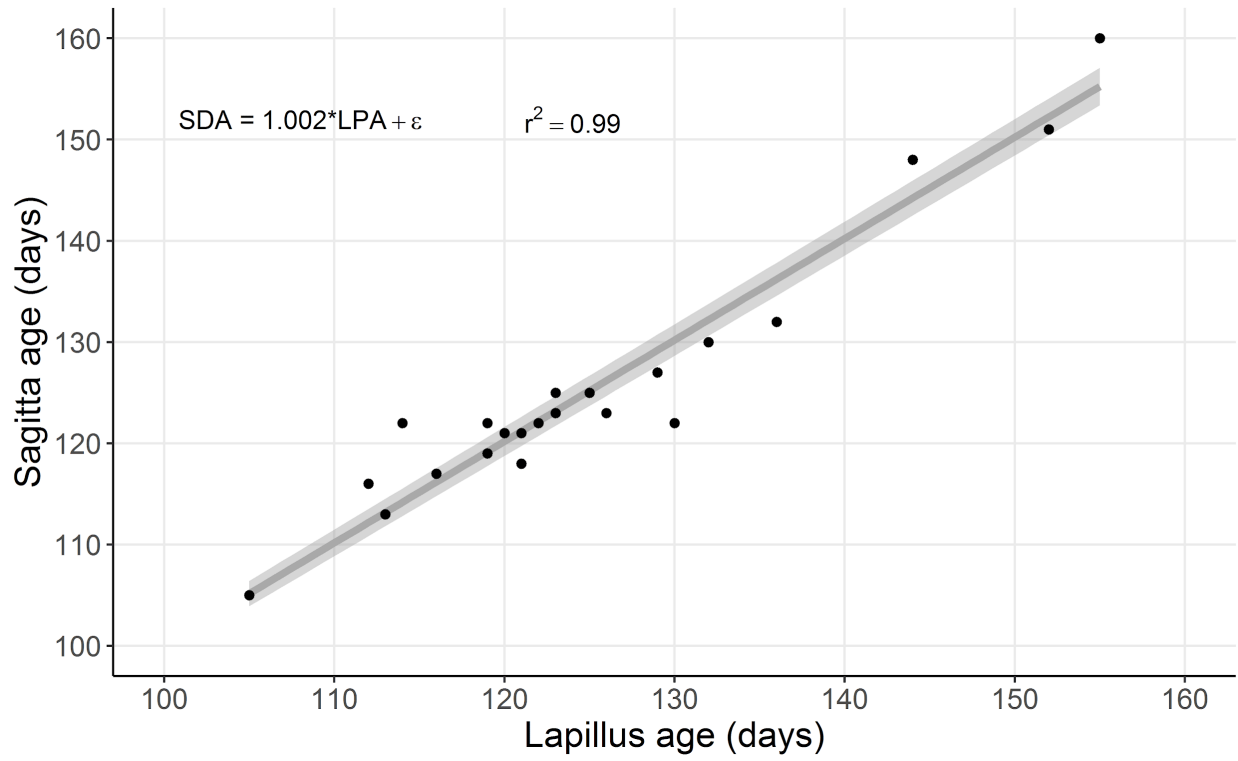


Figure 3. Paired daily ages estimated using lapillar and sagittal otoliths of juvenile sablefish sampled during August of 2014 and 2016.

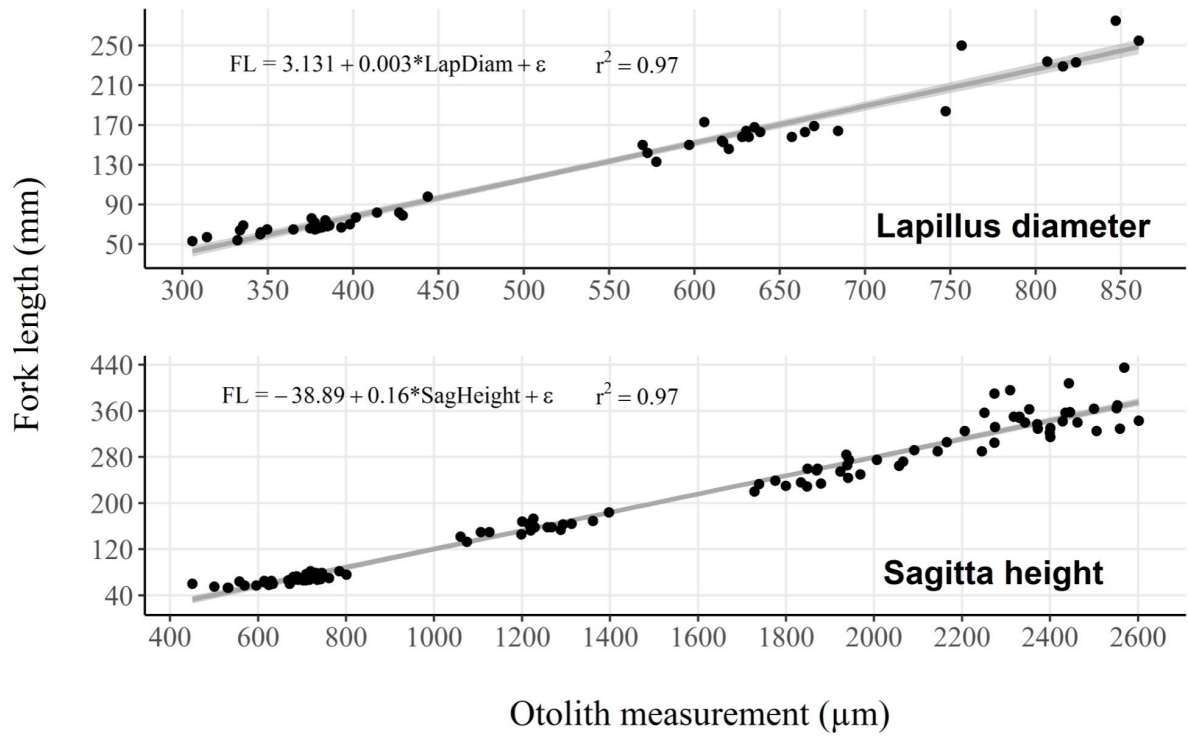


Figure 4. Linear models of lapillar otolith diameter and sagittal otolith height against juvenile sablefish fork length of age-zero fish sampled from July through October of 2017.

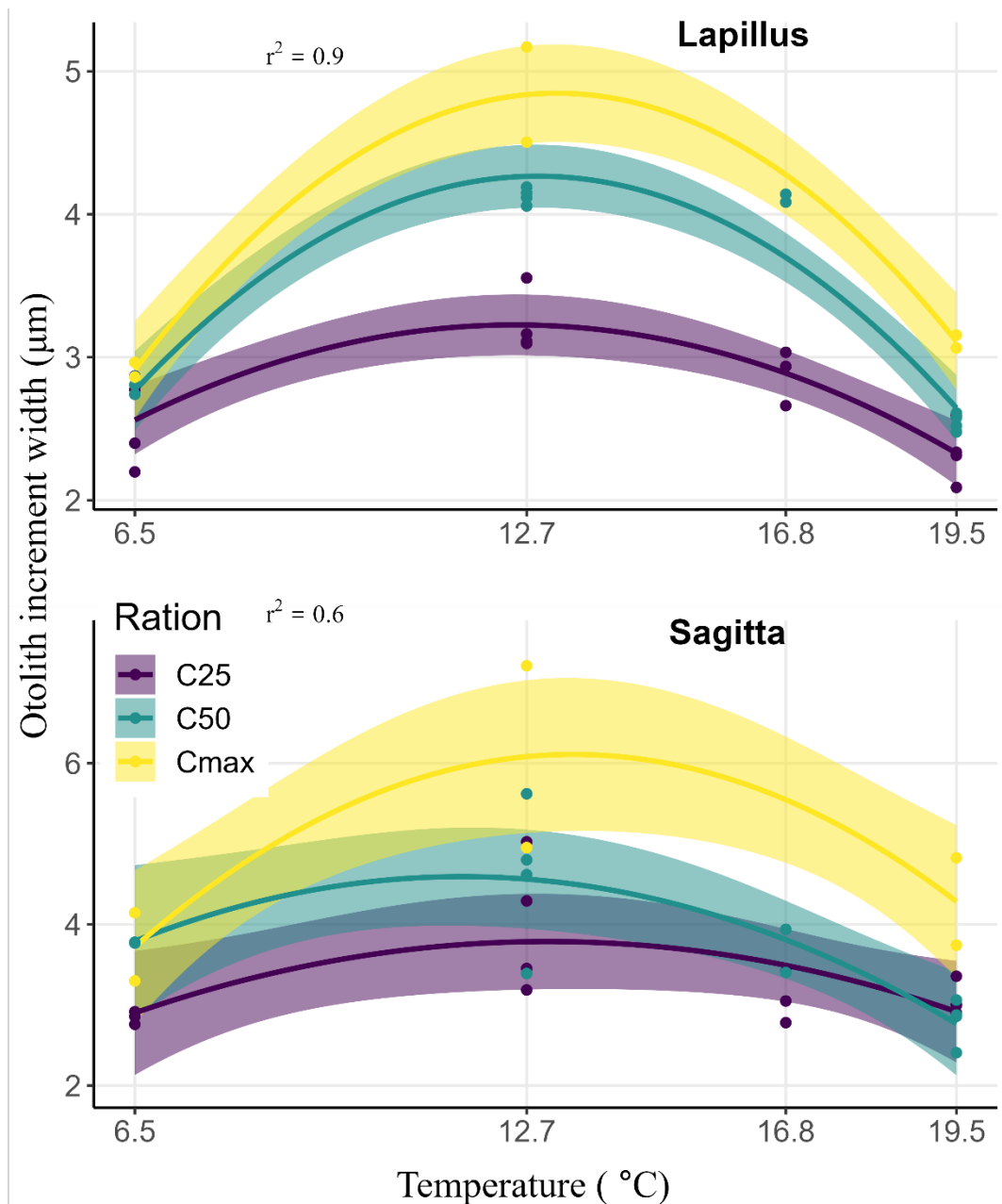


Figure 5. Average daily increment widths of lapillus and sagitta collected from juvenile sablefish reared in varying temperature and feed-ration trials. Lines and intervals represent fitted quadratic equations and 95% confidence intervals. Increments were only measured during the last 30 days of the trial.

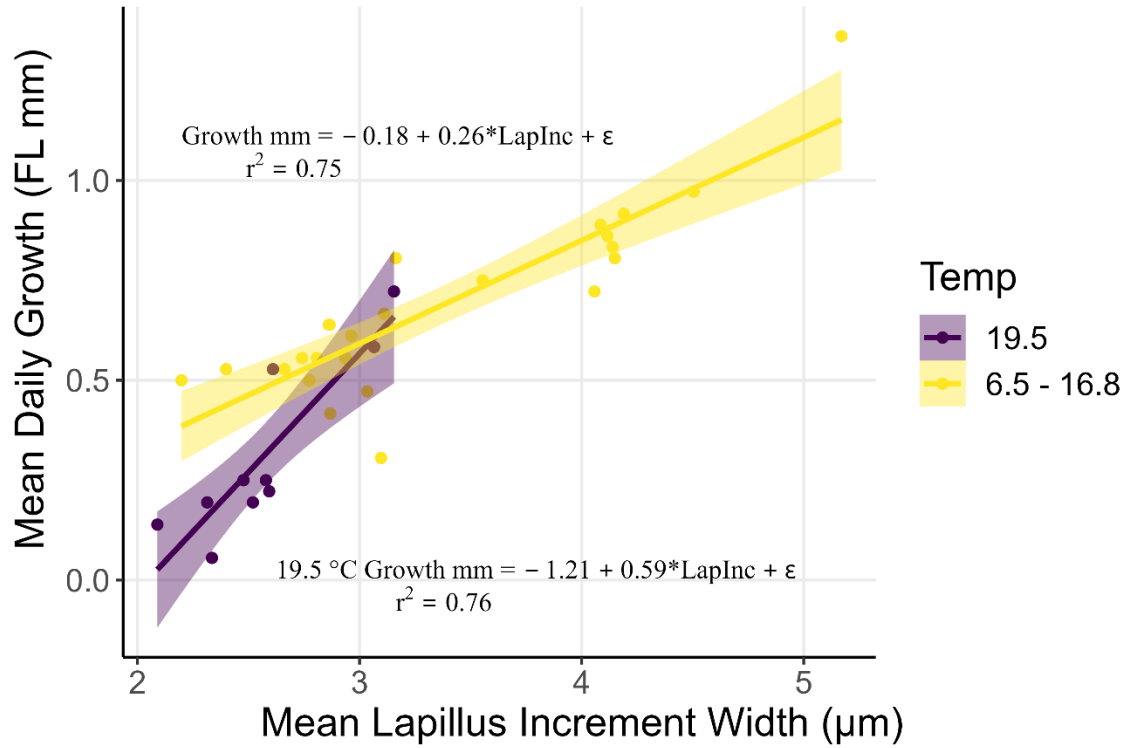


Figure 6. Observed mean daily juvenile sablefish fork length (FL) growth vs. mean daily lapillus increment width across temperature treatments. A significantly different slope (more steep) was only observed at 19.5 °C and only within the lapillus.



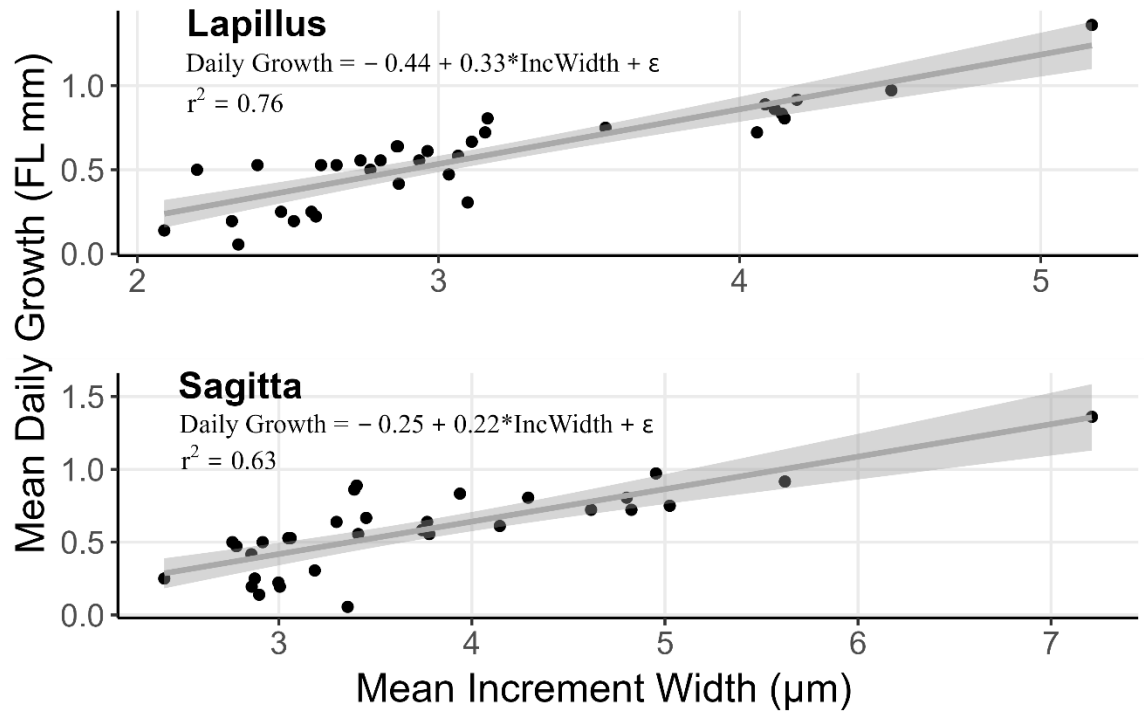
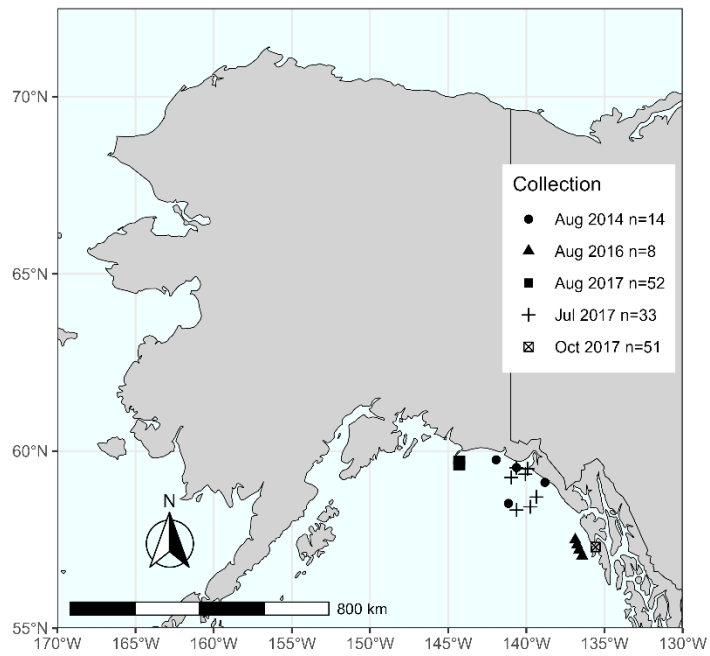


Figure 7. Observed mean daily juvenile sablefish fork length (FL) growth vs. mean daily increment width for both structures.



Supplemental Figure 1. Collection map by month and year demonstrating the location of capture and number of individuals used for this study.